Scaling the fluctuation of the flow capacity of core logs in a formation in southeastern Mexico

S. Matias-Gutierres

Department of Environmental Engineering, Instituto Tecnológico de Estudios Superiores del Oriente del Estado de México, Tecamachalco, Los Reyes Acaquilpan, 56400, State of México, México. Applied Research In Earth Science, 06700, Cuauhtémoc CDMX, México.

E. I. García-Otamendi

Department of Information Technologies, Universidad Autónoma del Estado de Hidalgo, Highway Tizayuca-Pachuca Km. 2.5, Tizayuca, CP. 43800, Hidalgo, México.

H. D. Sánchez-Chávez

Institute of Physics and Mathematics, Universidad Tecnológica de la Mixteca, Km.2.5 Highway to Acatlima, Huajuapan de León, 69000, Oaxaca, México.

R. Cifuentes-Villafuerte

Grupo "Mecánica Fractal", Instituto Politécnico Nacional, CDMX, 07738, México.

Received 25 January 2024; accepted 27 November 2024

This study evaluates flow capacity fluctuations in well cores from a southeastern Mexico formation using PDPK^i records. Petrophysical measurements provide wellbore wall flow capacity data, used to identify trends. Applying a dynamic scaling approach akin to the Family-Vicsek method, we analyze discrete kh^* records. In particular, the order parameter structure function q was applied to the flow capacity records, and the exponents characterizing dynamic scaling α, β, z were identified, revealing self-affine scalings for fluctuations. Data collapse of flow capacities occurs in the northern zone with higher fractures and oil production, contrasting with the poorly collapsed flow capacity in the southern zone. This suggests superior flow capacity in fractal reservoir media compared to Euclidean counterparts.

Keywords: Flow capacity; structure function; fluctuation; collapse.

DOI: https://doi.org/10.31349/RevMexFis.71.030602

1. Introduction

The fluid flow capacity in porous media, influenced by rock formations (oil or gas reservoirs), is defined as the product of the equivalent permeability K and the thickness H_F of the formation. This parameter plays a crucial role in assessing reservoir potential and various reservoir engineering calculations. The flow capacity, challenging and costly to characterize, depends on the mobility or permeability of the fluid in the porous rock medium, controlled by intrinsic factors such as diversity in pore structures (matrix, cavities, and fractures), connectivity between them [1], flow path tortuosity [2–4], sedimentation, diagenesis, and drilling-induced formation damage [5–10]. In the oil industry, the estimation of the flow capacity, KH_F, of the formation or reservoir is commonly assessed through the Darcy equation. Subsequently, pressure and production tests in the reservoir are the primary means of estimation for determining this parameter [10–12]. Responses in pressure and production transients vary based on fluid flow dynamics and formation geometry [13–15]. Similarly, local measurements and their petrophysical interpretation are used to infer the predominant type of medium in the formation.

In Euclidean or fractal analysis, theoretical models are applied to infer general characteristics. For instance, Euclidean analysis considers single, double, or triple porosities [16,17], while fractal analysis is addressed in [13,18–21]. Therefore, for manifestations of the Euclidean type, it is possible to determine an equivalent or average permeability, K, of the system in the radial flow interval, corresponding to the height H_F of the formation under study in the pressure test. This allows for the estimation of the flow capacity of the formation. While, in the case of fractal geometry, the response follows power-law behaviors. Therefore, an equivalent or average permeability is often not estimated since the pressure transient does not stabilize, making it unfeasible to estimate the flow capacity. Typically, in this type of fractal analysis, permeability functions are presented concerning dimensionless radial distance and various fractal parameters such as connectivity dimension [22], backbone dimension, chemical dimension, etc., as demonstrated in previous studies [13, 14, 19, 20, 23]. Although these studies are limited by deterministic fractal derivations, they are crucial for characterizing the formation and calibrating petrophysical models in fluid flow simulations.

Therefore, various models have been proposed for the assessment of flow capacity based on well logs, considering variables such as matrix porosity, vugs, and fissures [7], water saturation and shale volume in the formation [24], dolomitization [10], and so forth. The use of scalar logs at the core and well levels is a common practice that has demonstrated that certain formations exhibit fractal structures in their composition. Examples include textures in core images, the diversity of pores observed in cores, fractures, stratigraphy, and seismic faults. These processes exhibit scaling behavior and are classified by fractal dimensions [25–29]. As for scalar logs of oil and gas flow capacity at the well level, they are often employed to plot their cumulative curve against depth (h_{deep}) and identify flow units that characterize specific rock types [12]. The importance of characterizing flow capacity locally is reflected in studies that employ different scaling processes to infer it [9, 10, 30–34].

In this study, we propose to employ the dynamic scaling approach of Family-Vicsek [35] to investigate whether universal fluctuation dynamics emerge in the formation and/or diffusion process of the reservoir, measured at a local scale within the field, across various test wells located in different productive sites in southeastern Mexico. The spatial scale invariance is assessed through the series of flow capacity roughness records provided by discrete log-well measurements of kh_{deep} over a total sample size of length L. This roughness is weighted through the standard deviation $w(L,t)$ of $h(x,t)$.

The structure of the current paper is as follows. Section 2 provides a brief overview of the study area and general information about the geology of the utilized records. Section 3 outlines the methodology based on the dynamic scaling theory of Family Vicsek, with mathematical details applied to the analysis of scalar records of kh to identify fluctuations associated with flow capacity records. Section 4 describes the obtained results and discusses their interpretation. Finally, the conclusions of this study are presented.

2. Area and study data

The study area encompasses two carbonate reservoir regions in southeastern Mexico: one in the northwest (**NW**) and the other in the southeast (**SE**), as illustrated in Fig. 1. The primary facies observed in both regions include dolomitized floatstone and rudstone with varying degrees of fracturing and dissolution, generating cavities of different sizes. For this study, two series of kh flow capacity records were used in each region, respectively labeled as **ZN1**, **ZN2**, for the northern region, and **ZS1**, **ZS2**, for the southern region, designated in this manner for confidentiality reasons. In general, from the petrophysical geological analysis of cores, it was determined that in the **NW** zone, dolomites with hydrocarbon impregnation are observed, showing abundant fracturing in various directions with good remaining porosity and partially open fracturing. For the **SE** Zone, microdolomite is present in portions. Additionally, there is little partially open fracturing observed. It is considered a more brecciated region, although not uniformly, it exhibits sedimentological variations that could influence diagenetic variations. The (**NW**) zone appears to have high hydraulic capacity and corresponds to higher hydrocarbon production, while the (**SE**) zone shows lower production capacity.

3. Methodology

Commonly, the Family Vicsek interface growth model is widely used for time series associated with economic, seismic, biological, physical, geological systems, etc. [36–39]. The purpose of applying this methodology is based on finding the spatial and temporal dependence of the fluctuation associated with the time series records. This dependence is showed by scaling the statistical moment (roughness or standard deviation of the series records when $q = 2$) as a function of the interface heights relative to the length L or size of the time series.

The Family-Vicsek dynamic scaling model associated with fluctuations in the heights $h(x,t)$ of rough interfaces $w(L,t)$ implies a generic scaling invariance with respect to the space-time variables L and t, respectively. This is quantified by critical exponents α, β, z that arise from the dynamic scaling law of roughness given in Eq. (1) [35].

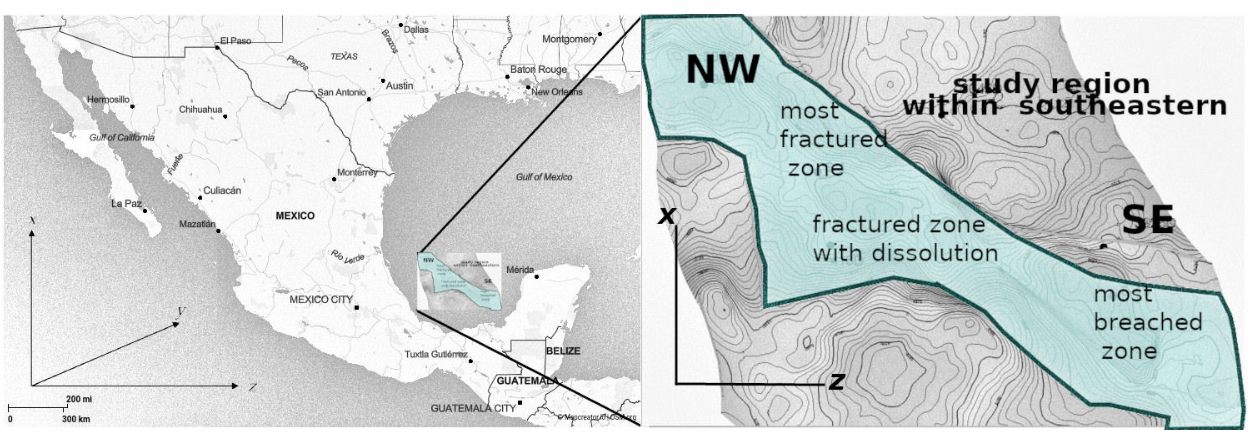

FIGURE 1. Distribution of flow capacity records in the central region of the study area within the southeastern part of Mexico.

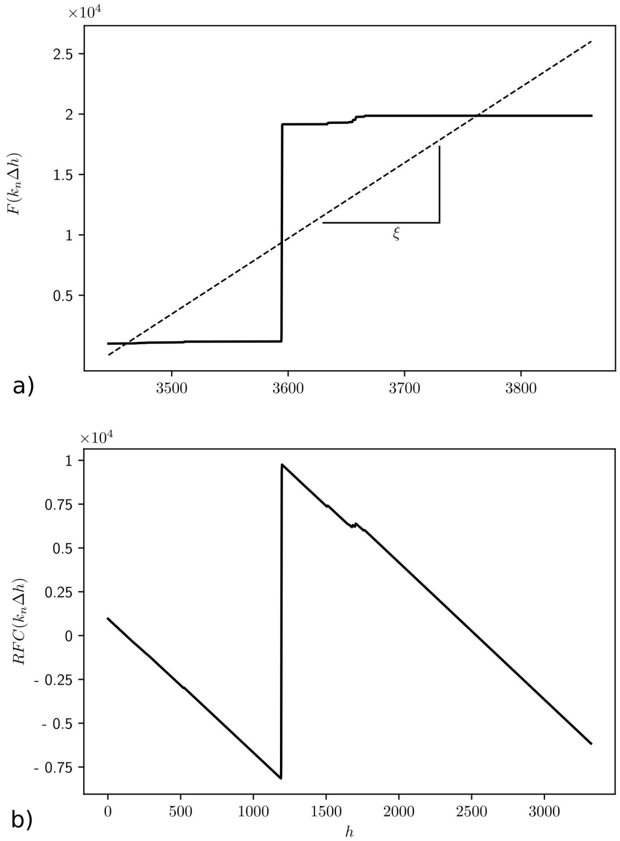

FIGURE 2. a) Cumulative flow capacity curve $F(k_n\Delta h)$ vs depth of the records h_{deep} (solid line), linear fit (dashed line). b) Fluctuation function vs depth.

$$w_q(\delta_n) = \begin{cases} L^\alpha & t^* << t \\ t^\beta & t << t^* \end{cases}. \tag{1}$$

The w_q is called the generalized function of the $q-th$ moment. It is expressed as follows,

$$w_q = \langle |h_{n+\delta_n} - h_n|^q \rangle \,, \tag{2}$$

where the angular brackets $\langle \ldots \rangle$ represent an ensemble average over all pairs of points separated by a distance δ_n, which is a natural number in the interval $[1, N-1]$. N represents the length of the series. Then, the absolute values of $N-\delta_n$ for all pairs of points given by $(h_n, h_{n+\delta_n})$ are calculated. The mean of the set is approximated using the arithmetic mean.

$$w_q(\delta_n) = \left(\frac{1}{N-\delta_n} \sum_{n=1}^{N-\delta_n} |h_{n+\delta_n} - h_n|^q \right)^{1/q} , \tag{3}$$

where α is referred to as the roughness or Hurst exponent, characterizing the behavior of the series. β denotes the growth exponent of the series, and the ratio $z = \alpha/\beta$ is termed the dynamic exponent. This dynamic exponent is utilized to identify characteristic times at which the interface width $w(L,t)$ reaches saturation. The relationship between the system size L and the critical saturation time t^* is expressed as $t^* \sim L^z$. The interfaces will exhibit either self-affine or self-similar geometry depending on the nature and magnitude of these exponents [41].

For this study, series of scalar flow capacity records were utilized to determine the associated fluctuation. The methodology applied to the wellbore wall flow capacity records quantifies a measure in which the qth order structure functions describe the scale dependence of expected values of the qth moment (statistical moments). Drawing information from the petrophysical and geological interpretation of the analyzed wells, discrete scalar flow capacity records given by $k_n\Delta h$, where $\Delta h = h^*$, are considered. Subsequently, the cumulative flow capacity is constructed as $F(k_n\Delta h) = \sum_{i=1}^{n} k_i\Delta h$, and this curve is associated with a fit given by the linear relation $\xi_F = \xi \cdot k_n\Delta h$ [see Fig. 2a)]. Then, it is possible to construct the fluctuation function, which we will refer to as the relative flow capacity (RFC). This function is obtained from the cumulative curve of $k_n\Delta h$ with respect to its linear fit and is mathematically expressed as follows in Eq. (3), [see Fig. 2b)].

$$RFC(k_n\Delta h) = F(k_n\Delta h) - \xi \cdot k_n\Delta h. \tag{4}$$

4. Empirical results and discussion

To analyze the RFC [see Fig. 2b)], we employ the metric of the order parameter structure function q [Eq. (3)]. If the system exhibits correlations, one would expect $w_q(\delta_n)$ to display power-law behavior, $w_q \propto (\delta_n)^{\alpha_q}$, where α_q represents the Generalized Hurst exponent H_q [46].

We found that the q-order structure functions of the Relative Flow Capacity (RFC) records exhibit power-law behavior for well ZN1 with $\alpha_q = \alpha = 0.95 \pm 0.01$ at least for $1 \leq q \leq 5$, as shown in Fig. 4a) and detailed in Table I. This indicates a self-affine characterization of the RFC [41]. Subsequently, a self-correlation through power-law scaling for the RFC concerning depth is presented, parallel to the vertical direction on the y-axis of the sampled records. These exponents are of the same order as those found for sandstone samples from geological environments that exhibit permeability fluctuations while maintaining long-range correlations with exponent $H_y \approx 0.90$ for permeability records [47].

The scaling exponents for the additional wells within the two designated study zones (refer to Fig. 1) pertain to the northwest and southeast regions of the Mexican area, are shown in Table I, where self-affinity is observed, indicating that the processes exhibit long-range memory and characterize these two regions. Statistical persistence has also been observed in well records for lithofacies characterization through the multifractal approach and the calculation of the Hurst exponent [42]. However, for other reservoirs in different regions of the world, short-term memory processes have been found using the rescaled range analysis (R/S) approach [43].

This naturally does not contradict our results but presents an additional parameter for studying the heterogeneities of the formation. On the other hand, the universality of classes

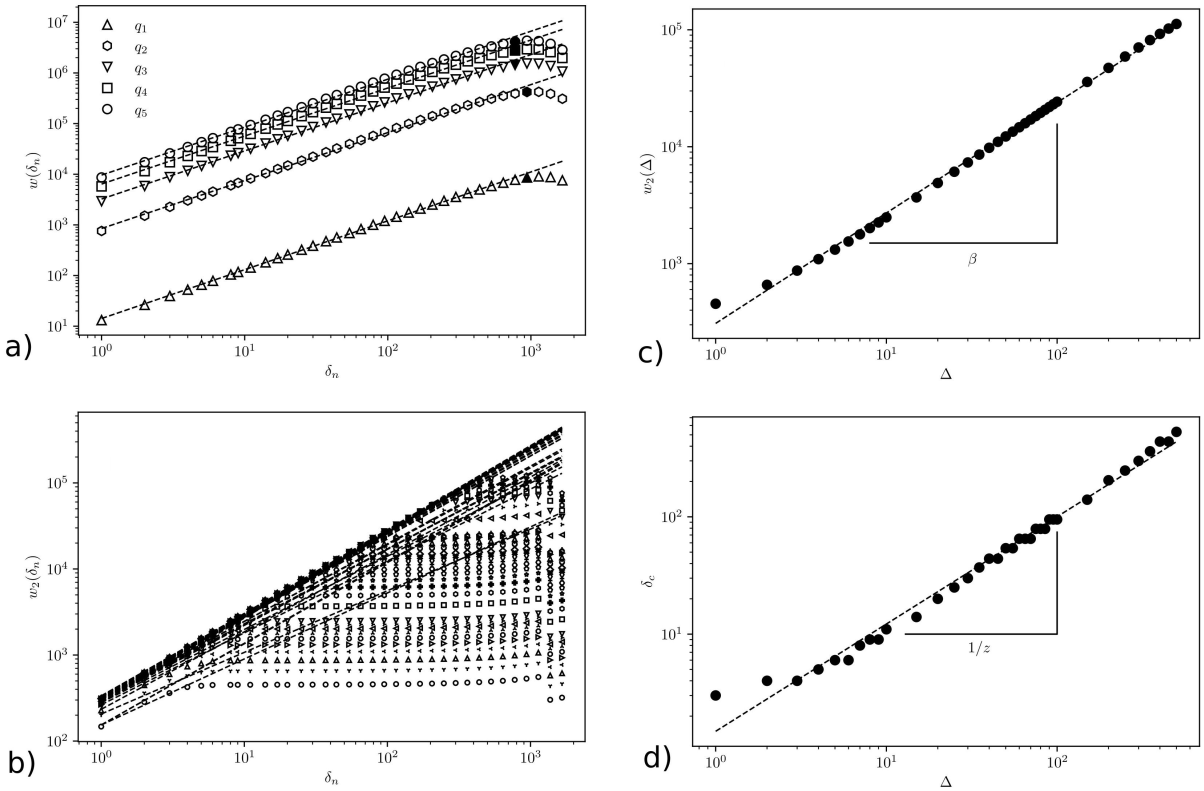

FIGURE 3. a) Structure function (well **ZN1**). b) Dynamic structure function $w(\delta_q)$ vs Δ_n. c) Log-log plot of $w_2(\delta_n < \delta_c, \Delta)$ vs size intervals Δ, well ZN1. d) Log-log correlation plot with δ_c intervals against Δ intervals, well ZN1.

TABLE I. q-order structure function (exponent α_q).

Records of wells		$w_q \propto (\delta_n)^{\alpha_q}$				
		q				
		1	2	3	4	5
well ZN1	$\alpha_q =$	0.96	0.94	0.95	0.94	0.94
well ZN2	$\alpha_q =$	0.94	0.93	0.92	0.93	0.93
well ZS1	$\alpha_q =$	0.72	0.76	0.76	0.76	0.76
well ZS2	$\alpha_q =$	0.82	0.81	0.82	0.82	0.81

in diffusion and fluid flow processes is evident when we observe that the scaling exponent for well **(ZN1)** is almost similar to that obtained for geophysical porosity records with $q = 2$ by [44] (obtained by the Multifractal Detrended Fluctuation Analysis (MFDFA) approach) and for seismic trace records near wells [45]. The latter authors associate the multifractality of porosity records to the significant influence of shale presence and variations in the subsurface sedimentation pattern, suggesting that the presence of gas in reservoir zones weakens the multifractal behavior of porosity records.

On the other hand, the dynamics of fluctuations are studied by constructing new flow capacity profiles parallel to the y-axis, based on the initial flow capacity records. To achieve this, the following function with respect to n as the spatial variable and the sampling width Δ as the temporal variable is used: $h(n,\Delta) = \sqrt{(1/\Delta)\sum_{k=n-\Delta+1}^{n}(A_k - \langle A_k\rangle)^2}$. It depicts the fluctuations of a dynamic interface within the $x-y$ plane. To determine the exponent β, the structure function is applied to these flow capacity profiles. This function should exhibit power-law behavior where the values scale with the sampling intervals as follows: $w_2(\Delta, \delta_n < \delta_c) \propto \Delta^\beta$, and the structure functions scale with the window width δ_n.

The power-law behavior is displayed in Fig. 3c) for well **ZN1** with $\beta = 0.944$, and for the other records from the study areas, the scaling behavior of the structure functions concerning δ_n is established, and the results for β are shown in Table II. This exponent β indicates a correlation of the structure function with what could be a temporal evolution of the medium. However, as in [36], we observe a spatial correlation with respect to the x-axis. Additionally, scaling is observed to be maintained over three orders of magnitude.

Subsequently, it is necessary to determine the coefficient z, called the dynamic exponent. We plot $\log\delta_c$ vs $\log\Delta$, expecting $\delta_c \propto \Delta^{1/z}$. From the graph in Fig. 3d), we find that $z = 1.09$ for well **ZN1**, and the other z exponents are shown in Table II. While good vertical correlations with α (along the Y direction) and horizontal correlations with β (along the X direction) have been demonstrated, it is possible to visualize cross-correlation with respect to both the x and y axes. Finally, a collapse of information is observed in Fig. 4 with coordinates of the structure function $f = w_2/\Delta_n^\beta$ and win-

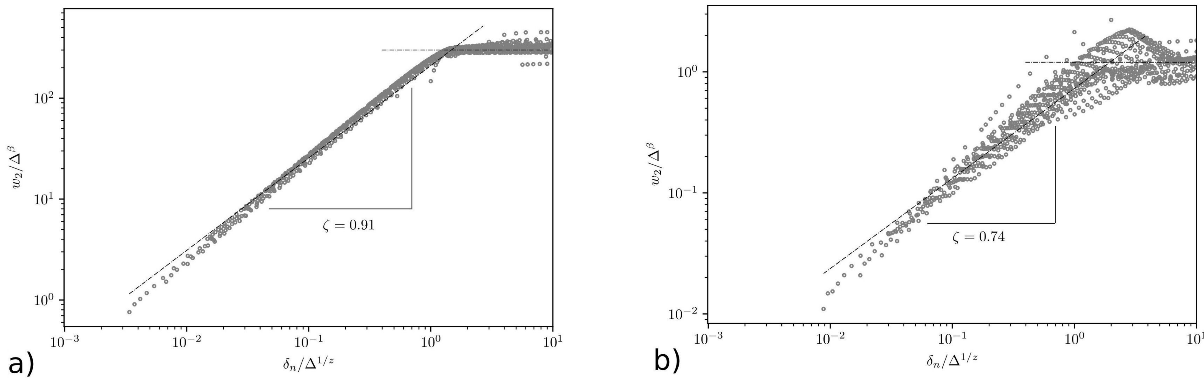

FIGURE 4. "Dynamic exponent ζ": Data collapse according to the dynamic scaling coordinates w_2/Δ^β vs $\delta_n/\Delta^{1/z}$, where ζ, $\beta = z\zeta$ are the dynamic scaling exponents of Family-Vicsek [49].

TABLE II. Characteristic exponents of Family-Vicsek.

Area		exponents		
		Roughnes	Growth	Dynamic
		$\alpha,\ q=2$	β	z
Northeast	well ZN1	0.947	0.944	1.09
	well ZN2	0.933	0.944	1.143
Southeast	well ZS1	0.765	0.600	1.313
	well ZS2	0.819	0.724	1.158

dow width $\delta_n/\Delta_n^{1/z}$. The exponent z is determined from the plots of $\log f$ vs $\log \delta_n/\Delta_n^{1/z}$ and is shown in Table II for the two study areas.

From Figs. 3d), 4, and Table II, we observe that only for the wells in the northern part, there is clear information collapse [Fig. 4a)], indicating good vertical and horizontal autocorrelation. In other words, the medium exhibits well-defined fractal behavior. This is not the case for wells in the southern zone, where, although there are good independent correlations in both the vertical and horizontal directions, as shown in Fig. 4b) -the collapse plot of information-, there is no apparent cross-correlation, at least in the $x - y$ plane of the mobile interfaces. In other words, the medium exhibits a more Euclidean behavior. This implies that the medium exhibits more Euclidean behavior in the southern zone. This observation is associated with the structure of the medium; the reservoirs in the northern zone have fractal porous media, showcasing higher oil production and better flow capacity. Conversely, the reservoirs with a Euclidean structure in the southern zone exhibit lower oil production and reduced flow capacity. Similar behavior was reported by [48] in an experimental comparative study of water discharge in Euclidean and fractal reservoirs. In their study, the fractal reservoir model was an inverse pre-fractal of the Menger sponge, and the Euclidean medium was modeled by a translationally invariant network of square rectangles. They found that the discharge from the Menger sponge was greater than that from the Euclidean medium.

5. Conclusions

After characterizing the flow capacity fluctuation profile for the two study zones in Mexico, it has been observed that the analyzed wells in zones **ZN** and **ZS** exhibit long-range behavior with self-affine scaling up to three orders of magnitude for flow capacity fluctuations. This scaling follows the vertical direction along the y axis, which aligns with the depth of the records. Similarly, the autocorrelation along the x axis is established with the growth exponent β, determining the exponent for the moving interface fluctuations. The exponent z reveals the cross-correlation between the α and β exponents, and an information collapse is observed. The northern zone is noted for its increased fracturing, hydraulic flow capacity, and information collapse. In contrast, the southern zone, with fewer fractures and lower hydraulic flow capacity, shows no information collapse. This leads to the conclusion that zone **ZS** represents a more homogenous, Euclidean-like medium, whereas zone **ZN** is more heterogeneous, with a fractal behavior better defined by its exponents. In other words, if the structure is fractal in the $x - y$ direction and crosswise, it corresponds to better flow capacity. Ultimately, this finding could contribute to the local characterization of reservoirs with the goal of reconstructing the modeling of the petrophysical property matrix, where the local heterogeneity of the medium is preserved.

i. Pressure-Decay Profile Permeameter (PDPK-400), provides a precise method for rapidly determining core permeability and heterogeneity. These data can be used to identify and quantify thin, highly permeable beds, permeability barriers, and depositional/diagenetic features. It measures the permeability automatically in both Y and X-axis on up to 3 meters of core at one time.

1. C. Wang, X. Liu, E. Wang, M. Wang, and C. Liu, Dependence of connectivity dominance on fracture permeability and influence of topological centrality on the flow capacity of fractured porous media. *Journal Of Hydrology*. **624** (2023) 129883, `https://doi.org/10.1016/j.jhydrol.2023.129883`
2. B. Ghanbarian, A. Hunt, R. Ewing, and M. Sahimi, Tortuosity in Porous Media: A Critical Review. *Soil Science Society Of America Journal*. **77** (2013) 1461, `https://onlinelibrary.wiley.com/doi/full/10.2136/sssaj2012.0435`
3. Y. Jin, Y. Zhu, X. Li, J. Zheng, and J. Dong, Scaling Invariant Effects on the Permeability of Fractal Porous Media. *Transport In Porous Media*. **109** (2015) 433, `https://doi.org/10.1007/s11242-015-0527-4`
4. S. Coleman, and J. Vassilicos, Transport properties of saturated and unsaturated porous fractal materials. *Physical Review Letters*. **100** (2008) 035504, `https://doi.org/10.1103/PhysRevLett.100.035504`
5. J. Qiao *et al.*, Insights into the pore structure and implications for fluid flow capacity of tight gas sandstone: A case study in the upper paleozoic of the Ordos Basin. *Marine and Petroleum Geology*. **118** (2020) 104439, `https://doi.org/10.1016/j.marpetgeo.2020.104439`
6. B. Beall, R. Tjon-Joe-Pin, and H. Brannon, Progressive Technology Increases Flow Capacity in Horizontal Wells. *Proceedings - SPE Eastern Regional Conference And Exhibition*. **10** (1997) 161, `https://dx.doi.org/10.2118/39230-MS`
7. N. Bona, F. Radaelli, A. Ortenzi, A. Poli, C. Peduzzi, and M. Giorgioni, Integrated Core Analysis for Fractured Reservoirs: Quantification of the Storage and Flow Capacity of Matrix, Vugs, and Fractures. *SPE Reservoir Evaluation and Engineering*. **6** (2003) 226, `https://dx.doi.org/10.2118/85636-PA`
8. J. Klotz, R. Krueger, and D. Pye, Effect of Perforation Damage on Well Productivity. *Journal Of Petroleum Technology*. **26** (1974) 1303, `https://dx.doi.org/10.2118/4654-PA`
9. M. N. Acharya *et al.*, Flow Path Characterization: A Deterministic Approach for Reconciliation of Flow Capacity Changes from Matrix and Fractures Productivity in Deep Jurassic Reservoirs in North Kuwait. *Proceedings-SPE Annual Technical Conference And Exhibition*. **4** (2013) 3181, `https://dx.doi.org/10.2118/166347-MS`
10. M. N. Acharya *et al.*, Flow Capacity Evaluation in a Complex Carbonate Reservoir: Key to Understand Reservoir Productivity and Stimulation Effectiveness. *Proceedings - SPE Annual Technical Conference And Exhibition*. **1** (2012) 267, `https://dx.doi.org/10.2118/156101-MS`
11. J. A. Barker, generalized radial flow model for hydraulic tests in fractured rock. *Water Resources Research*. **24** (1988) 1796, `https://doi.org/10.1029/WR024i010p01796`
12. P. Balossino, F. Pampuri, C. Bruni, and K. A. Ebzhasarova, New Integrated Approach to Obtain Reliable Permeability Profiles From Logs in a Carbonate Reservoir. *SPE Russian Oil And Gas Technical Conference And Exhibition 2006*. **1** (2006) 453, `https://dx.doi.org/10.2118/102289-MS`
13. J. Chang, and Y. Yortsos, Pressure-Transient Analysis of Fractal Reservoirs. *SPE Formation Evaluation*. **5** (1990) 31, `https://dx.doi.org/10.2118/18170-PA`
14. A. Balankin, and B. Elizarraraz, Map of fluid flow in fractal porous medium into fractal continuum flow. *Phys. Rev. E - Statistical, Nonlinear, And Soft Matter Physics*. **85** (2012) 056314, `https://doi.org/10.1103/PhysRevE.85.056314`
15. A. Balankin, J. Valdivia, J. Marquez, O. Susarrey, and M. Solorio-Avila, Anomalous diffusion of fluid momentum and Darcy-like law for laminar flow in media with fractal porosity. *Physics Letters A*. **380** (2016) 2767 `https://doi.org/10.1016/j.physleta.2016.06.032`
16. J. Warren, and P. Root, The Behavior of Naturally Fractured Reservoirs. *Society Of Petroleum Engineers Journal*. **3** (1963) 245, `https://dx.doi.org/10.2118/426-PA`
17. D. Abadassah, and I. Ershaghi, Triple-Porosity Systems for Representing Naturally Fractured Reservoirs. *SPE Formation Evaluation*. **1** (1986) 113, `https://dx.doi.org/10.2118/13409-PA`
18. H. Park, J. Choe, and J. Kang, Pressure Behavior of Transport in Fractal Porous Media Using a Fractional Calculus Approach. *Energy Sources*. **22** (2010) 881, `https://doi.org/10.1080/00908310051128237`.
19. J. A. Acuna, I. Ershaghi, and Y. C. Yortsos, Practical Application of Fractal Pressure-Transient Analysis in Naturally Fractured Reservoirs. *SPE Formation Evaluation*. **10** (1995) 173, `https://dx.doi.org/10.2118/24705-PA`.
20. F. Flamenco-López, and R. Camacho-Velázquez, Determination of Fractal Parameters of Fracture Networks Using Pressure-Transient Data. *SPE Reservoir Evaluation and Engineering*. **6** (2003) 39, `https://dx.doi.org/10.2118/82607-PA`
21. L. Fanhua, and L. Ciqun, Pressure-transient analysis of two-layers fractal reservoirs. *Applied Mathematics And Mechanics (English Edition)*. **19** (1998) 21, `https://doi.org/10.1007/BF02458977`
22. K. Razminia, A. Razminia, and D. Torres, Pressure responses of a vertically hydraulic fractured well in a reservoir with fractal structure. *Applied Mathematics And Computation*. **257** (2015) 374, `https://doi.org/10.1016/j.amc.2014.12.124`
23. B. O'Shaughnessy, and I. Procaccia, Analytical Solutions for Diffusion on Fractal Objects. *Physical Review Letters*. **54** (1985) 455, `https://doi.org/10.1103/PhysRevLett.54.455`
24. B. Sinanan, Integrated Petrophysical Approach Fast-tracks Development and Results From a Heavy-Oil Reservoir in Trinidad. *Proceedings - SPE Latin American and Caribbean*

Petroleum Engineering Conference. (2005), https://dx.doi.org/10.2118/94490-MS

25. C. Barton, and P. Pointe, Fractals in Petroleum Geology and Earth Processes. (Springer US, 1995). https://doi.org/10.1007/978-1-4615-1815-0
26. F. Jestczemski, and M. Sernetz, Multifractal approach to inhomogeneous fractals. *Physica A: Statistical Mechanics And Its Applications*. **223** (1996) 275, https://doi.org/10.1016/0378-4371(95)00365-7
27. S. Havin and A. Bunde, Fractals in Science (Springer-Verlag, 1994).
28. H. Hardy and R. Beier, Fractals in Reservoir Engineering (World Scientific, 1994).
29. C. Barton, R. Paul and P. La Pointe, Fractals in the Earth Sciences, Vol. 53 (New York: Plenum Press, 1995).
30. V. Rios, L. Santos, and D. Schiozer, Upscaling Technique for Highly Heterogeneous Reservoirs Based on Flow and Storage Capacity and the Lorenz Coefficient. *SPE Journal*. **25** (2020) 1981, https://dx.doi.org/10.2118/200484-PA
31. S. Gómez *et al.*, Well Test Analysis of Naturally Fractured Vuggy Reservoirs with an Analytical Triple Porosity - Double Permeability Model and a Global Optimization Method. *Oil and Gas Science And Technology - Revue D'IFP Energies Nouvelles*. **69** (2014) 653, https://doi.org/10.2516/ogst/2013182.
32. M. Lozada-Zumaeta *et al.*, Distribution of petrophysical properties for sandy-clayey reservoirs by fractal interpolation. *Nonlinear Processes In Geophysics*. **19** (2012) 239, https://doi.org/10.5194/npg-19-239-2012,2012
33. A. Verma, P. Kumar, W. Mohant, A. Routray, and B. Cheadle, Modeling of reservoir property using fractal interpolation and geostatistics. *SEG Technical Program Expanded Abstracts*. **33** (2014) 2460, https://library.seg.org/doi/10.1190/segam2014-1567.1
34. T. Babadagli, Effective permeability estimation for 2-D fractal permeability fields. *Mathematical Geology*. **38** (2006) 33, https://doi.org/10.1007/s11004-005-9002-z
35. F. Family, and T. Vicsek, Scaling of the active zone in the Eden process on percolation networks and the ballistic deposition model. *Journal Of Physics A: Mathematical And General*. **18** (1985) L75, https://dx.doi.org/10.1088/0305-4470/18/2/005
36. A. Balankin, D. Matamoros, J. Ortiz, M. Ortiz, E. León, and D. Ochoa, Scaling dynamics of seismic activity fluctuations. *Europhysics Letters*. **85** (2009) 39001, https://dx.doi.org/10.1209/0295-5075/85/39001
37. Y. Ezaier, A. Hader, A. Latif, L. Amallah, I. Achik, and Y. Boughaleb, Morphological properties of the interfaces growth of composite membranes. *Materials Today: Proceedings*. **66** (2022) 238, https://doi.org/10.1016/j.matpr.2022.03.729
38. K. Fujimoto, R. Hamazaki, and Y. Kawaguchi, Family-Vicsek Scaling of Roughness Growth in a Strongly Interacting Bose Gas. *Physical Review Letters*. **124** (2020) 210604, https://doi.org/10.1103/PhysRevLett.124.210604
39. S. Ouadfeul, and L. Aliouane, Multifractal Analysis Revisited by the Continuous Wavelet Transform Applied in Lithofacies Segmentation from Well-Logs Data. *International Journal Of Applied Physics And Mathematics* **1** (2011) 10, https://doi.org/10.7763/ijapm.2011.v1.3.
40. F. Family, and T. Vicsek, Scaling of the active zone in the Eden process on percolation networks and the ballistic deposition model. *Journal Of Physics A: Mathematical And General*. **18** (1985) L75, https://dx.doi.org/10.1088/0305-4470/18/2/005
41. P. Meakin, Fractals, scaling, and growth far from equilibrium, **vol. 5** (Cambridge University Press, 1998).
42. E. Hernández-Martinez, T. Perez-Muñoz, J. Velasco-Hernández, A. Altamira, and L. Velasquillo, Electrofacies Recognition from Well-Log Data . An R/S Scaling Analysis Approach. *Submitted Mathematical Geosciences* **45** (2013) 471. https://doi.org/10.1007/s11004-013-9445-6.
43. R. Rahimi, M. Bagheri, and M. Masihi, Characterization and estimation of reservoir properties in a carbonate reservoir in Southern Iran by fractal methods. *Journal Of Petroleum Exploration And Production Technology*. **8** (2018) 31, https://doi.org/10.1007/s13202-017-0358-7
44. D. Subhakar, and E. Chandrasekhar, Reservoir characterization using multifractal detrended fluctuation analysis of geophysical well-log data. *Physica A: Statistical Mechanics And Its Applications*. **445** (2016) 57, https://doi.org/10.1016/j.physa.2015.10.103
45. H. Elyas, H. Hossein, S. Yousef, and J. Seyed, Self-similar segmentation and multifractality of post-stack seismic data. *Petroleum Exploration And Development*. **47** (2020) 781, https://doi.org/10.1016/S1876-3804(20)60093-3
46. H. Peitgen, H. Jürgens, and D. Saupe, Chaos and Fractals. *Chaos And Fractals* (1992).
47. H. Makse, S. Havlin, P. Ivanov, P. King, S. Prakash, and H. Stanley, Pattern formation in sedimentary rocks: Connectivity, permeability, and spatial correlations. *Physica A: Statistical Mechanics And Its Applications*. **233** (1996) 587, https://doi.org/10.1016/S0378-4371(96)00246-4
48. A. Balankin, L. Morales-Ruiz, S. Matías-Gutierres, O. Susarrey-Huerta, D. Samayoa-Ochoa, and J. Patiño-Ortiz, Comparative study of gravity-driven discharge from reservoirs with translationally invariant and fractal pore networks. *Journal Of Hydrology*. **565** (2018) 467, https://doi.org/10.1016/j.jhydrol.2018.08.052
49. A. Barabási and H. Stanley, Fractal Concepts in Surface Growth (Cambridge University Press, 1995).